Crystallization Kinetics and Morphology in Phase Separating and Sedimenting Mixtures of Colloidal Spheres and Rods

S. M. Oversteegen,* J. G. E. J. Wijnhoven, C. Vonk, and H. N. W. Lekkerkerker

Van't Hoff Laboratory for Physical and Colloid Chemistry, Debye Research Institute, Utrecht University, P.O. Box 80051, 3508 TB Utrecht, The Netherlands

Received: February 25, 2004; In Final Form: July 23, 2004

The crystallization of sedimentating silica spheres in the presence of silica-coated boehmite rods in low-salt dimethylformamide is studied by means of confocal scanning laser microscopy. As expected, addition of rods gives rise to a net attraction due to the depletion effect. Upon increasing rod volume fractions, below a predicted equilibrium binodal, crystalline ordering of the spheres takes place faster but gives cause for more grain boundaries. Addition of rods at volume fractions in the theoretically predicted two-phase region gives rise to aggregation and glasslike sediments. We explain these results on the basis of the different gravitational lengths and sedimentation rate of both species: higher rod concentrations drive the system quicker into the two-phase region of the predicted phase-diagram.

I. Introduction

The stability of suspensions such as coatings, containing spherical pigments, can change drastically when rodlike particles, frequently used as rheology enhancers, are added. Mixtures of rods and spheres may also arise naturally in the synthesis of pigments. Their phase behavior may greatly influence the way the pigments can be processed in, e.g., color filters or fillings. The mutual asymmetry of the colloids alone may already induce a net attraction between alike particles by the so-called depletion effect.[1−3] The closer the hard spheres are together, the more volume is available to the rods. In this manner, the system may gain more conformational freedom and hence a higher, more favorable, entropy. This depletion effect has been well-established both theoretically and experimentally for bimodal mixtures of colloidal spheres,[4] colloidal mixtures of spheres and polymers,[5] platelets and polymers,[6−8] and rods and platelets.[9−11]

When a rod enters the gap between two hard spheres that are nearer than the length of the rod, the former can no longer assume all conformations, as illustrated in Figure 1. This unfavorable loss of entropy can be overcome by depleting the rod from the gap thereby gaining orientational realization probabilities. When outnumbered, the consequent lower density of rods between the spheres may give rise to an unbalanced osmotic pressure amid the spheres and forces the latter together. The strength of this "attraction through repulsion" or depletion potential W reads up to first order in the rod density ϕ_r[12−14]

$$\frac{W(h)}{k_B T} = -\frac{1}{3}\phi_r \frac{L}{D}\frac{\sigma}{D}\left(1-\frac{h}{L}\right)^3 \qquad (1.1)$$

Here h is the face-to-face distance of the spheres of diameter σ, whereas L represents the length of the rod and D its diameter, as indicated in Figure 1a. Moreover, k_B is the Boltzmann constant and T the absolute temperature. In the appropriate limits, i.e., low density and relatively small rods ($L \ll \sigma$), eq 1.1 has been confirmed experimentally.[15−17]

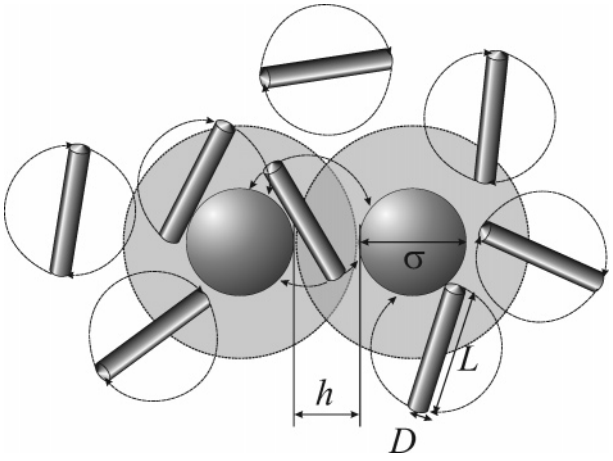

Figure 1. An unbalanced pressure between two spheres arises since the rods that are closer to a sphere than half their length cannot rotate freely. This creates a net attraction between the spheres.

For certain rod concentrations, the net attraction of the spheres may be large enough to induce phase separation. This has been predicted by means of the free-volume theory[18] applied to spheres and rods[19,20] and has indeed been observed in colloidal mixtures of spheres and rods.[21−24] All these experimental studies observe the depletion interaction "as is". However, the kinetics in these phase-separating systems in relation to sedimentation has not been studied yet but is nevertheless of great importance to the above-mentioned applications. In this paper, we therefore have a closer look on the kinetics and the final sediments of phase-separating sedimenting colloidal spheres in the presence of colloidal rods.

II. Experimental Section

We prepare silica spheres and silica-coated boehmite rods. When dispersed in dimethylformamide (DMF), the van der Waals interactions between the spheres are negligible since the

* To whom correspondence may be addressed. E-mail: m.oversteegen@chem.uu.nl.

10.1021/jp0491515 CCC: $27.50
Published on Web 10/28/2004

refractive indices of silica and DMF are closely matched. Although DMF does not match with boehmite, the interactions of the silica-coated rods may in a good approximation considered to be hard, in analogy to previous studies.[22,23] Residual charges are screened by the addition of little salt. Moreover, since the refractive indices of the silica (coated) particles and DMF are close to each other, the mixtures are very suitable to be examined in real space by means of confocal laser scanning microscopy (CSLM).[25] To be able to do so, we incorporate a dye in the core of the spherical particles. An uncolored silica shell is synthesized around this core to have silica interactions only and to distinguish individual particles in the analysis of the CSLM pictures. This two-step synthesis method has first been successfully developed by van Blaaderen and Vrij.[26]

In section IIA, we first describe how the spheres and rods are synthesized and analyzed. Subsequently, we specify how the samples are prepared in section IIB.

A. Synthesis and Analysis. FITC-Labeled Silica Spheres. Before preparing the core, fluorescein isothiocyanate (FITC) is chemically bound to 3-(aminopropyl)triethoxysilane (APS) where the latter acts as a coupling agent between silica and FITC. The number of FITC molecules per sphere must comply with two requirements. On one hand, the number of dye molecules must be sufficient to make the particles visible using CSLM, whereas on the other, a too high dye concentration may give rise to autobleaching.[27] Both requirements are met when typically 10^6 FITC/APS dimers[28,29] are build in into each core following the well-known Stöber synthesis[30] using tetraethoxysilane (TEOS). The size of the core of a base-catalyzed Stöber synthesis can be chosen by adding the appropriate amount of ammonia, as indicated in Appendix A.

We must meet two opposite demands for the desired size of our cores. Because of the relatively large density of porous silica ($\sim 2 \times 10^3$ kg/m^3) as compared to DMF ($\sim 0.9 \times 10^3$ kg/m^3), the spheres will sediment fast. By taking small sizes, the sedimentation can best be followed in time using the microscope. However, the optical resolution of the microscope ($\sim$300 nm), prevents us from taking very small spheres. Both requirements come toward each other by taking 9.8 vol % of 25% aqueous ammonia in ethanol. The synthesized cores were analyzed using transmission electron microscopy (TEM). By analyzing 162 particles from TEM micrographs, we find 676 nm cores in diameter.

Subsequently, a thin shell is grown around the prepared cores to a desired size. To that end, the appropriate amount of TEOS is added. The final particles were analyzed by means of both static light scattering (SLS) and TEM. From SLS data gathered on a FICA 50 photometer thermostated at 25 °C, we obtained a diameter of 723 ± 36 nm. We finally found from 136 particles on TEM micrographs the spheres to be 700 ± 44 nm in diameter.

Silica-Coated Boehmite Rods. The rods are synthesized by coating boehmite rods with silica. For the boehmite (γ-AlOOH) synthesis, we adopted the method as developed by Buining et al.[31,32] in which the size of hydrothermally grown fibrils can be tuned. Aluminum alkoxides are dissolved in acidified double-distilled water and treated at 150 °C.

The coating of the boehmite particles with silica is realized here by titrating the dispersion of pH = 5−6 with a 3 w/w% solution of sodium silicate (pH = 11).[33−35] The negatively charged silica particles (isoelectric point (IEP) of 2.0) deposit on the positively charged surface of the boehmite rods (IEP of 9.2) until a monolayer is formed. The deposition of the silica particles then stops because of repulsion of the negatively charged silica particles. The boehmite dispersion is very dilute (typically 1 kg/m^3), and the titration is carried out under ultrasonication and vigorous stirring to prevent aggregation of the particles. Moreover, the pH of the dispersion is kept between 9 and 10 by adding a resin. This also prevents dissolution of the silica. After titration, the dispersion is dialyzed for 9 days against demineralized water to remove excess silicate. When dialysis is prolonged, eventually silica will be removed from the boehmite particles. The silica-coated boehmite rods have been analyzed by TEM, yielding a length of the rods of $L = 118$ nm and a diameter of $D = 13.9$ nm both with a polydispersity of about 30%.

B. Sample Preparation. The particles are transferred from the Stöber mixture into DMF with 1 mM LiCl, suppressing the double layer to about 10 nm thickness,[28,23] by repeated centrifugation. By means of an Anton Paar DMA 5000 density meter, the densities of the solvent and particles were determined. The density of the solvent (DMF + 1 mM LiCl) is close to the one in the literature for pure DMF, 948 and 944 kg/m^3, respectively. However, both the measured (viscosity-corrected) densities of the prepared core/shell silica-spheres (2099 ± 5 kg/m^3) and the silica-coated boehmite rods (2562 ± 24 kg/m^3) seem slightly too high. The systematic higher values may be due to some little contamination in the density meter left from previous measurements. We will nevertheless use the values found as their influence on the position in the phase diagram will not change dramatically.

By drying and weighing known amounts of the stock dispersions of the spheres and rods, we determined the respective volume fractions from the previously measured densities. The stock solution of the core/shell silica spheres in DMF/1 mM LiCl looks clear and orange and fully sediments within a day. The dispersion of the rods is slightly turbid and very viscous. In both dispersions, the particles are stable against flocculation after two years since they easily redisperse after sedimentation. This suggests that the van der Waals attractions may indeed be neglected.

Samples of desired volume fractions were weighed from the stock dispersions and solvent in a test tube. After vigorous shaking on a vortex, approximately 1 mL of the sample was transferred by a Pasteur pipet into a vial from which the bottom was replaced by a microscope cover slip of 0.11 mm thickness. The vial was subsequently placed onto a Leica TCS NT (inverted) microscope in fluorescence mode, using a 488-nm Ar/Kr laser and an 100 × oil objective with a numerical aperture of 1.4. All confocal images are sized 512 × 512 pixels and taken within one second (top to bottom).

III. Results and Discussion

By use of free-volume theory,[18,20] we calculated the phase diagram using the experimental values for the dimensions of the particles, i.e., $\sigma = 700$ nm, $L = 118$ nm, and $D = 13.9$ nm. The predicted phase diagram is shown in Figure 2. The slanted tie lines connect the coexisting fluid (F) and crystal (C) phases of the spheres. Because of the double layer around the particles, the effective sizes may differ. Although this 10 nm may be negligible compared to the length of the rods and the diameter of the spheres, it is substantial relative to the diameter of the rods. However, it can be shown that this only has a minor effect on the phase diagram. It is seen from eq 1.1 ($\phi_r = (1/4)\pi D^2 L$) that this indeed is a second-order effect. The shape of the phase diagram is very reminiscent to that of the sphere/polymer mixtures,[5,36] albeit that the binodal for rods is lowered 1 order of magnitude as compared to polymers.

To be able to follow the crystallization due to sedimentation of the colloidal spheres, the initial volume fraction, that means

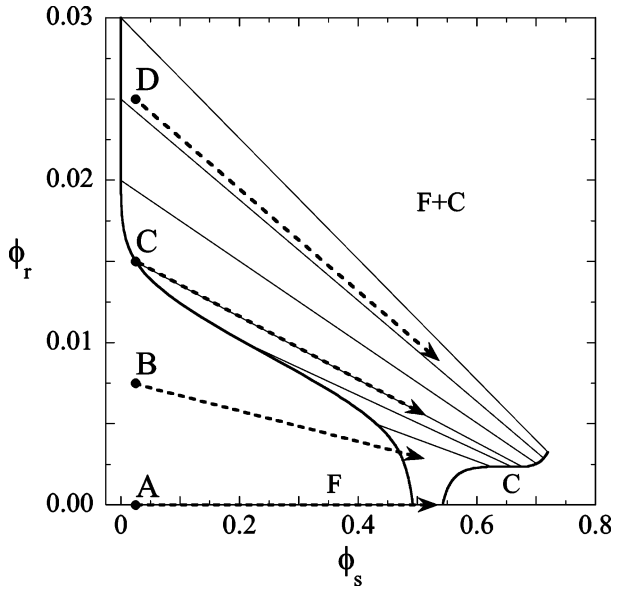

Figure 2. Calculated phase diagram for a mixture of spheres (σ = 700 nm) with spherocylinders (L = 118 nm, D = 13.9 nm). The slanted tie lines connect coexisting volume fraction of spheres, ϕ_s, and rods, ϕ_r, in the fluid (F) and crystal (C) phases. The dots labeled A−D indicate the position of the selected samples in the phase diagram prior to sedimentation. The dashed arrows point in what direction the volume fractions in the samples change through the theoretically predicted phase-diagram upon sedimentation at a given height in the sample.

prior to sedimentation, has to be taken rather low. In analogy to previous experiments,[36,37] we prepared all samples with an initial overall volume fraction of spheres of $\phi_s = 0.025$. We studied 15 samples of that volume fraction of spheres with an initial volume fraction of rods varying from $\phi_r = 0$ to $\phi_r = 0.03$. Despite the very low volume fractions of rods, this corresponds to an attraction up to $4k_BT$, according to eq 1.1. Here, we will discuss only four of those samples that represent the characteristics best. These samples are indicated A−D in Figure 2 on their initial position in the phase diagram, i.e., immediately after redispersion.

Immediately after redispersion, the particles start to sediment. A measure for the decay of the concentration as a function of height is the so-called gravitational length

$$\ell \equiv \frac{k_BT}{\Delta\rho v_p g} \tag{3.2}$$

where $\Delta\rho$ is the buoyancy-corrected density of the particle, v_p the particle's volume, and g the standard acceleration of free fall. Applying the above experimental values, we find for the spheres a gravitational length of $\ell_s = 2.0 \times 10^{-6}$ m and for the rods $\ell_r = 0.014$ m.

Another quantity of interest is the sedimentation rate

$$v = \frac{k_BT}{f} \tag{3.3}$$

Here f is the Stokes friction coefficient, which is for infinite dilution given as[38]

$$f = \begin{cases} 3\pi\eta\sigma & \text{spheres} \\ \dfrac{3\pi\eta L}{\ln\left(\dfrac{L}{D}\right) + 0.315} & \text{rods} \end{cases} \tag{3.4}$$

where $\eta \approx 10^{-3}$ Pa·s is the solvent's viscosity. From the above experimental values, we find for the sphere $v_s = 3 \times 10^{-7}$ m/s and for the rods $v_r = 6 \times 10^{-10}$ m/s. After 1 h, the spheres have traversed typically a millimeter, something the rods have overcome after one month.

The height of the vial used is approximately 0.01 m. Hence, the spheres will gradually sediment, whereas the rods will to a good approximation remain distributed over the whole sample during the scope of the experiment. When we focus on a particular height in the sample, the solvent with rods will be replaced by the sedimenting spheres. To a very good approximation, the relative volume available to the rods is given by[19]

$$\frac{V_{free}}{V_{total}} = (1 - \phi)\exp\left\{-\frac{3}{2}\frac{L}{\sigma}\frac{\phi}{1-\phi}\right\} \tag{3.5}$$

where ϕ is the local volume fraction of spheres. When the spheres start to crystallize due to sedimentation at a certain height, say at $\phi = 0.5$, according to eq 3.5, 38% of the initially available space is still accessible to the rods. The local volume fraction of rods has hence decreased to approximately 38% of its initial value. That is, at that particular height the sample will move through the equilibrium phase-diagram upon sedimentation almost along the slanted arrows as indicated schematically in Figure 2. It is believed that the underlying equilibrium free-energy landscape may indeed serve as a template for the dynamic system.[39]

The first sample considered, A, only contains spheres. After vigorous shaking, the sample is placed on the confocal microscope. By looking 10 μm above the bottom of the sample, i.e., five times the gravitational length, we saw the sediment slowly filling up in a random fashion as shown in the left column of Figure 3. Apart from Brownian motion, the sample did not change after 45 min, and we put it at rest for one month. It is seen from the upper left picture in Figure 4 that the particles were able to reorganize within one month and form a nice crystalline sediment containing some glasslike, disordered patches. By taking the Fourier transform of this picture, it is obvious that the system tends to form a single crystal given the 6-fold symmetry in the bottom row of Figure 4.

Sample B, containing $\phi_r = 0.75$ vol %, is predicted to be in the one-phase region but nevertheless shows different behavior than the previous one. The presence of rods first manifests itself by a higher viscosity, initially leading to slower sedimentation (top row Figure 3). Despite the higher viscosity, the sample rapidly forms densely packed structures as can be explained from the phase diagram, Figure 2. Because of the presence of rods, the fluid-crystal equilibrium opens up, which drives the spheres quicker into the two-phase region. After one month, there are more crystalline domains in the sediment, as shown in Figure 4. However, there are also more grain boundaries present as it can be seen from the accompanying Fourier transform. The "scattering" pattern is more powderlike than without rods.

These effects are even more pronounced in sample C (ϕ_r = 1.50 vol %) close to the calculated binodal. The even higher viscosity does not prevent the fact that crystalline patterns are formed already within half an hour, as displayed in Figure 3. From Figure 4, it is seen that after one month no disordered patches are found. The crystalline areas are nevertheless smaller and there are consequently more grain boundaries. This is also reflected by the Fourier tranform that shows two full rings rather than separate spots previously. The faster crystallization of mixtures close to the binodal has also been observed in mixtures of spheres with (short) polymers.[36,40]

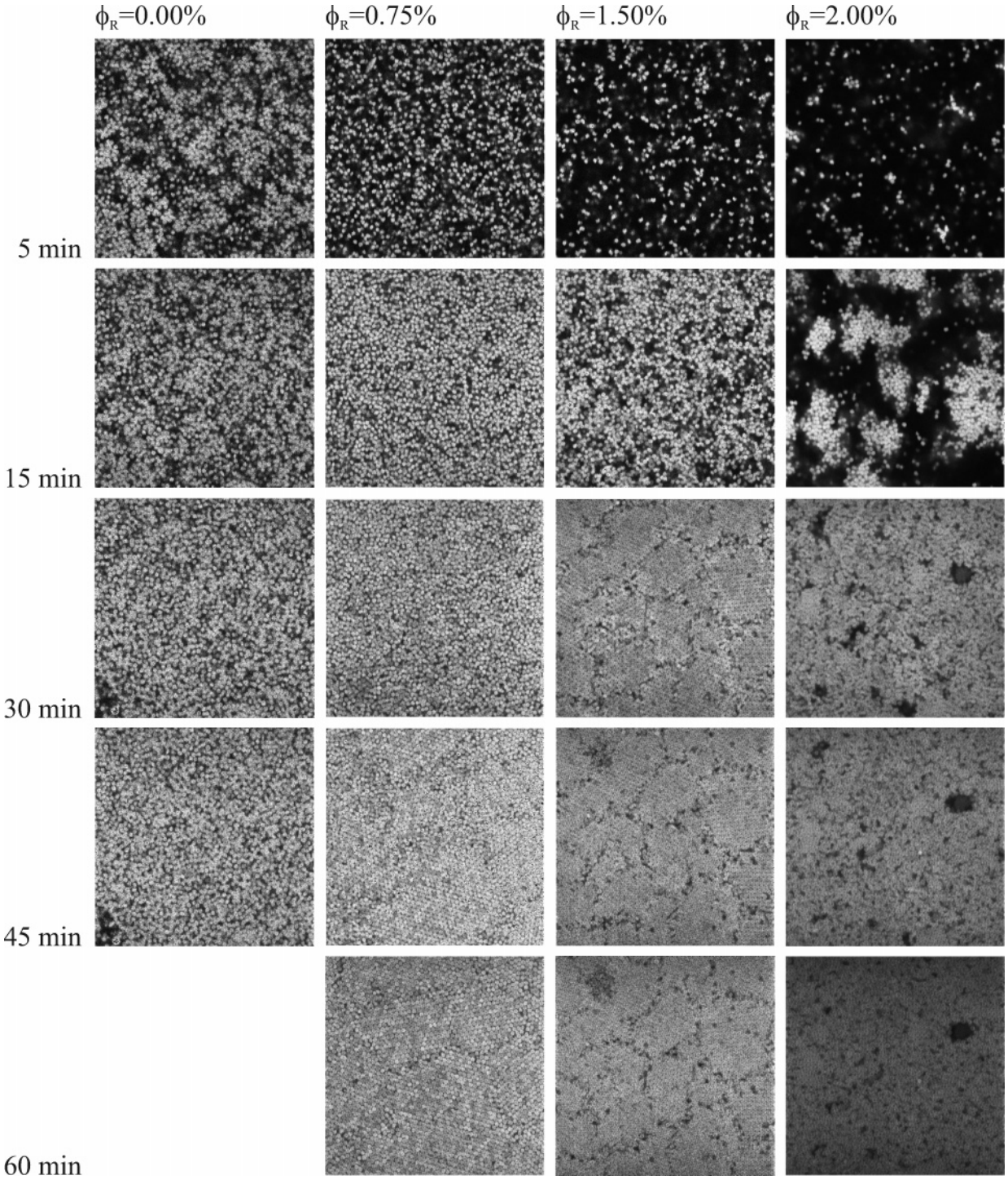

Figure 3. Confocal images of the samples A−D (left through right, cf. Figure 2) 10 μm from the bottom of the vial 5, 15, 30, 45, and 60 min (top to bottom) after redispersion.

With sample D, consisting of $\phi_r = 2.00$ vol % rods, we are immediately in the phase-separating region. Clearly the viscosity has gone up further as seen from the upper right picture in Figure 3. Nevertheless, aggregates of spheres are observed within a quarter of an hour. These large structures tumble down fast and form disordered structures. The system thus obstructs itself to crystallize within one month. Only small crystalline areas can be found in Figure 4. This is again very reminiscent of the sphere/polymer mixtures where in the two-phase region close to the binodal reaction limited cluster aggregates are formed,[41] but they are not able to reorganize.[40] The disorder in the eventual sediment is also seen from the Fourier transform, where no bright spots or rings can be distinguished.

The particle density has become too dense in this solvent to obtain a clear image 10 μm into the sample. Therefore, we took for each of the samples A−D four pictures in the sediment after one month at 5 μm above the bottom of the vial. A radial average of the intensities is taken from the Fourier transforms of the sediments, starting in the center of the images in Figure 4. These averages of intensities, $\langle I \rangle$, are shown in arbitrary units in Figure 5 as a function of the wavenumber k. For the samples A−C, two peaks are observed at the same spots, i.e., $k = 1.54$ and 2.71 μm^{-1}, indicated by the dotted lines. The ratio of these two values, $\sim\sqrt{3}$, suggests these are the $d_{(10)} = (1/2)\sigma\sqrt{3}$ and $d_{(11)} = (1/2)\sigma$ spacings, as depicted in the inset of Figure 5. Thus we obtain $\sigma = 750$ nm and $\sigma = 738$ nm, respectively. The

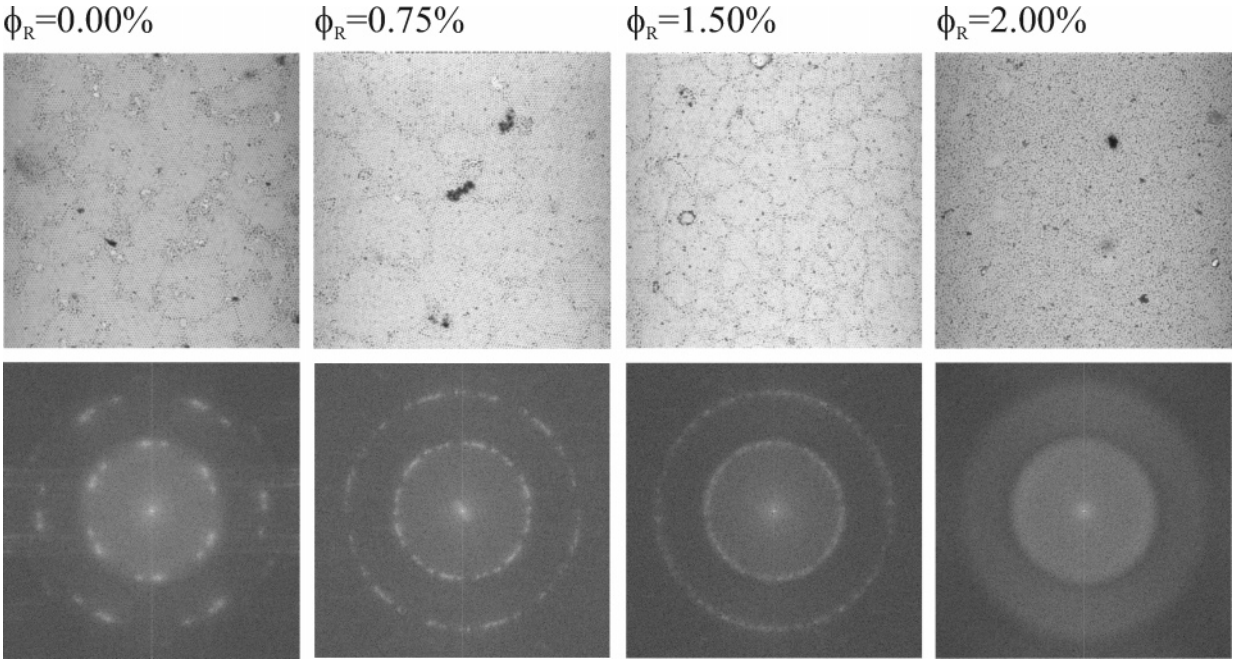

Figure 4. Confocal images of the sediments one month after redispersion 5 μm from the bottom of the vial in real space (top) and Fourier space (bottom). The samples A−D, as depicted in Figure 2, are given from left to right.

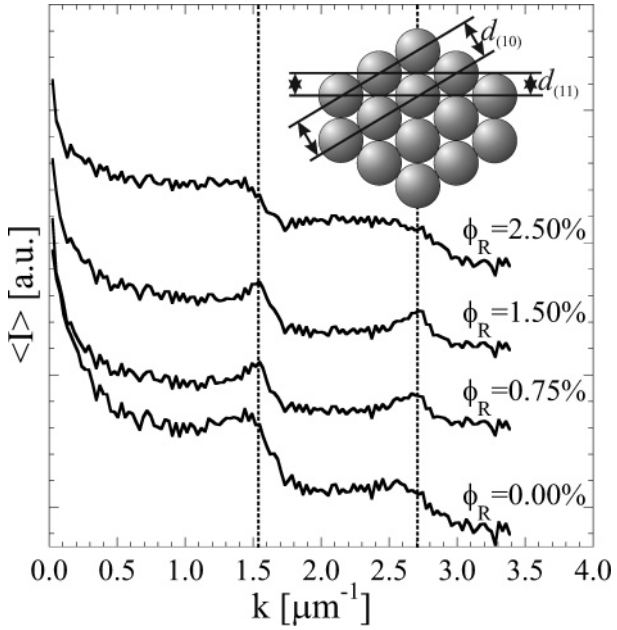

Figure 5. Radial averages of the intensity I of four Fourier transforms of the sediments of which one is depicted in Figure 4 for the samples A−D in Figure 2 (bottom through top). The first peak, indicated by the dotted line, stems from the $d_{(10)}$ spacing, whereas the second originates from $d_{(11)}$. For the aggregating sample D, the structure factor has vanished but the form factor is still clearly present.

discrepancy between these two values is in the order of the polydispersity of the particles (22 nm). The deviation from the bare diameter (700 nm) possibly indicates the presence of residual charges. It has indeed been found that the thickness of the double layer is in the order of 10 nm.[23,28]

The peaks are not observed in sample D, but a step in the intensity can nevertheless clearly be found at those spots. This is due to the fact that the Fourier transform contains both a structure and a form factor. Although the structure has vanished in the sediment of sample D, the shape of the form factor must still be present as the colloids touch in the disordered system.

In previous studies,[22,23] the depletion effect was not observed for $\phi_r > 0.6$ vol %, presumably due to the size of the capillaries used. Here, using 2 mL vials, we were able to prepare samples of rod concentrations up to $\phi_r = 3$ vol %. Above that volume fraction, the rod suspensions became highly viscous or even gelly. This prevented us from going deep into the two-phase region, further from the binodal. In analogy to sphere/polymer mixtures, one would expect diffusion-limited cluster aggregation, forming open stringlike fractal structures.[36,41] With less material than in sphere/polymer suspensions, the sphere/rod mixtures would then be a nice and cheaper alternative in, e.g., coating materials, since rods are rheological enhancers at the same time.

IV. Conclusions

On the basis of a combination of the equilibrium phase diagram and the sedimentation rate, the influence of the presence of rods on the sedimentation of colloidal spheres is studied. From free-volume theory, we obtained a phase diagram that is reminiscent to that found for sphere/polymer mixtures. However, phase transitions are expected at very low rod concentrations, which makes rods very effective depletion agents.

As with sphere/polymer mixtures, low volume-fractions of the rods in the vicinity of the binodal ($\phi_r < 0.015$) promote early crystalline ordering of the spheres. This, however, also leads to more grain boundaries and more powderlike structures due to the fact that intermediate rod concentrations force the spheres quicker into the two-phase region of the phase diagram. In the calculated two-phase region ($0.015 < \phi_r < 0.030$), fast reaction-limited cluster aggregation is observed and disordered sediments are obtained. The structures are kinetically arrested, and this obstructs crystallization. Experimental limitations prevented us from observing open fractal diffusion-limit cluster aggregates.

The Fourier transform of images of the sediments clearly shows the structure in the one-phase region. The tranforms may prove to be a valuable tool to locate the two-phase region experimentally where only the form factor remains. This reinforces our believe that the equilibrium phase-diagram may

provide a useful foundation to explain the origin of the dynamic phenomena observed.

Acknowledgment. S.M.O. thanks Dirk Aarts and Andrei Petukhov for their help and discussions on the interpretation of the Fourier images. The authors are grateful to Arnout Imhof, Jacob Hoogenboom, and Alfons van Blaaderen of the Soft Condensed Matter group (University Utrecht) for assisting us with the CSLM measurements on their microscope. This work is part of the SoftLink research program of the "Stichting voor Fundamenteel Onderzoek der Materie (FOM)", which is financially supported by the "Nederlandse Organisatie voor Wetenschappelijk Onderzoek (NWO)".

Appendix A: Particle Size Control

The size of silica particles from a base-catalyzed Stöber synthesis[30] can be controlled by means of an appropriate ammonia concentration. This dependence has been studied in full detail by Bogush et al.[42] A typing error in the original paper and another in an excellent review on silica synthesis[43] initially gave us, however, the wrong size. The corrected formula for the diameter σ of the spheres as a function of the ammonia concentration from a fit to the pioneering work of Bogush reads

$$\sigma = P[H_2O]^2 \exp(-Q[H_2O]^{1/2}) \quad (1.1)$$

where

$$P = [TEOS]^{1/2}(82 + 151[NH_3] + 1200[NH_3]^2 - 366[NH_3]^3) \quad (1.2a)$$

$$Q = 1.05 + 0.523[NH_3] - 0.128[NH_3]^2 \quad (1.2b)$$

Here $[H_2O]$ is the water concentration in the reaction mixture, [TEOS] the initial concentration tetraethoxysilane (we use 0.17 M), and $[NH_3]$ the ammonia concentration. Note that, when using aqueous ammonia, $[H_2O]$ and $[NH_3]$ are dependent variables.

The actual size of the synthesized particles with a dye built-in will be slightly higher than calculated from eq 1.1. Because of an increased ionic strength in the presence of dye, the nuclei tend to aggregate. Since there are less nuclei available with the same amount of TEOS, larger particles will be formed.

References and Notes

(1) Asakura, S.; Oosawa, F. *J. Chem. Phys.* **1954**, *22*, 1255.
(2) Asakura, S.; Oosawa, F. *J. Polym. Sci.* **1958**, *32*, 183.
(3) Vrij, A. *Pure Appl. Chem.* **1976**, *48*, 471.
(4) Dijkstra, M.; van Roij, R.; Evans, R. *Phys. Rev. E* **1999**, *59*, 5744 and references therein.
(5) Tuinier, R.; Rieger, J.; de Kruif, C. G. *Adv. Colloid Interface Sci.* **2003**, *103*, 1 and references therein.
(6) Bates, M.; Frenkel, D. *Phys. Rev. E* **2000**, *62*, 5225.
(7) van der Kooij, F. M. Vogel, M.; Lekkerkerker, H. N. W. *Phys. Rev. E* **2000**, *62*, 5397.
(8) Zhang, S. D.; Reynolds, P. A.; van Duijneveldt, J. S. *Mol. Phys.* **2002**, *100*, 3041.
(9) van der Kooij, F. M.; Lekkerkerker, H. N. W. *Langmuir* **2000**, *16*, 10144.
(10) Wensink, H. H.; Vroege, G. J.; Lekkerkerker, H. N. W. *J. Chem. Phys.* **2001**, *115*, 7319.
(11) Varga, S.; Galindo, A.; Jackson, G. *Phys. Rev. E* **2002**, *66*, 011707.
(12) Auvray, L. *J. Phys.* **1981**, *42*, 79.
(13) Mao, Y.; Cates, M. E.; Lekkerkerker, H. N. W. *Phys. Rev. Lett.* **1995**, *75*, 4548.
(14) Mao, Y.; Cates, M. E.; Lekkerkerker, H. N. W. *J. Chem. Phys.* **1997**, *106*, 3721.
(15) Lin, K.; Crocker, J. C.; Zeri, A. C.; Yodh, A. G. *Phys. Rev. Lett.* **2001**, *87*, 088301.
(16) Lin, K.; Crocker, J. C.; Zeri, A. C.; Yodh, A. G. *Phys. Rev. Lett.* **2001**, *87*, 269902.
(17) Helden, L.; Roth, R.; Koenderink, G. H.; Leiderer, P.; Bechinger, C. *Phys. Rev. Lett.* **2003**, *90*, 048301.
(18) Lekkerkerker, H. N. W.; Poon, W. C. K.; Pusey, P. N.; Stroobants, A.; Warren, P. B. *Europhys. Lett.* **1992**, *20*, 559.
(19) Bolhuis, P. G.; Frenkel, D. *J. Chem. Phys.* **1994**, *101*, 9869.
(20) Vliegenthart, G. A.; Lekkerkerker, H. N. W. *J. Chem. Phys.* **1999**, *111*, 4153.
(21) Adams, M.; Dogic, Z.; Keller, S. L.; Fraden, S. *Nature* **1998**, *393*, 349.
(22) Koenderink, G. H.; Vliegenthart, G. A.; Kluijtmans, S. G. J. M.; van Blaaderen, A.; Philipse, A. P.; Lekkerkerker, H. N. W. *Langmuir* **1999**, *15*, 4693.
(23) Vliegenthart, G. A.; van Blaaderen, A.; Lekkerkerker, H. N. W. *Faraday Discuss.* **1999**, *112*, 173.
(24) Dogic, Z.; Frenkel, D.; Fraden, S. *Phys. Rev. E* **2000**, *62*, 3925.
(25) van Blaaderen, A.; Ruel, R.; Wiltzius, P. *Nature* **1997**, *385*, 321.
(26) van Blaaderen, A.; Vrij, A. *Langmuir* **1992**, *8*, 2921.
(27) Imhof, A.; Megens, M.; Engelberts, J. J.; de Lang, D. T. N.; Sprik, R.; Vos, W. L. *J. Phys. Chem. B* **1999**, *103*, 1408.
(28) Imhof, A.; van Blaaderen, A.; Dhont, J. K. G. *Langmuir* **1994**, *10*, 3477.
(29) Imhof, A.; Dhont, J. K. G. *Phys. Rev. E* **1995**, *52*, 6344.
(30) Stöber, W.; Fink, A.; Bohn, E. *J. Colloid Interface Sci.* **1968**, *26*, 62.
(31) Buining, P. A.; Pathmamanoharan, C.; Bosboom, M.; Jansen, J. B. H.; Lekkerkerker, H. N. W. *J. Am. Ceram. Soc.* **1990**, *73*, 2385.
(32) Buining, P. A.; Pathmamanoharan, C.; Jansen, J. B. H.; Lekkerkerker, H. N. W. *J. Am. Ceram. Soc.* **1991**, *74*, 1303.
(33) Philipse, A. P. *Colloids Surf. A* **1993**, *80*, 203.
(34) Philipse, A. P.; Nechifor, A. M.; Patmamanoharan, C. *Langmuir* **1994**, *10*, 4451.
(35) van Bruggen, M. P. B. *Langmuir* **1998**, *14*, 2245.
(36) de Hoog, E. H. A.; Kegel, W. K.; van Blaaderen, A.; Lekkerkerker, H. N. W. *Phys. Rev. E* **2001**, *64*, 021407.
(37) Vliegenthart, G. A.; van Blaaderen, A.; Lekkerkerker, H. N. W. *Faraday Discuss.* **1999**, *112*, 173.
(38) Dogic, Z.; Philipse, A. P.; Fraden, S.; Dhont, J. K. G. *J. Chem. Phys.* **2000**, *113*, 8368.
(39) Evans, R. M. L.; Poon, W. C. K.; Renth, F. *Phys. Rev. E* **2001**, *64*, 031403.
(40) Anderson, V. J.; Lekkerkerker, H. N. W. *Nature* **2002**, *416*, 811.
(41) Anderson, V. J.; de Hoog, E. H. A.; Lekkerkerker, H. N. W. *Phys. Rev. E* **2001**, *65*, 011403.
(42) Bogush, G. H.; Tracy, M. A.; Zukoski, C. F., IV. *J. Non-Cryst. Solids* **1988**, *104*, 95.
(43) Giesche, H. Hydrolysis of Silicon Alkoxides in Homogeneous Solutions. In *Surfactant Science Series*; Sugimoto, T., Ed.; Marcel Dekker Inc.: 2000, Vol. 92, pp 126−146.